SUPPORTING INFORMATION FOR:

One-pot terpolymerisation of CHO, CO_2 and *L*-lactide using chloride indium catalysts.

Marc Martínez de Sarasa Buchaca,[a] Felipe de la Cruz-Martínez,[a] Luis F. Sánchez-Barba,[c] Juan Tejeda,[a] Ana M. Rodríguez,[a] José A. Castro-Osma,[b] Agustín Lara-Sánchez.[a]**

[a] Universidad de Castilla-La Mancha, Departamento de Química Inorgánica, Orgánica y Bioquímica-Centro de Innovación en Química Avanzada (ORFEO-CINQA), Facultad de Ciencias y Tecnologías Químicas, 13071-Ciudad Real, Spain. E-mail: Agustin.Lara@uclm.es

[b] Universidad de Castilla-La Mancha, Departamento de Química Inorgánica, Orgánica y Bioquímica-Centro de Innovación en Química Avanzada (ORFEO-CINQA), Facultad de Farmacia, 02071-Albacete, Spain. E-mail: JoseAntonio.Castro@uclm.es

[c] Universidad Rey Juan Carlos, Departamento de Biología y Geología, Física y Química Inorgánica, 28933-Móstoles, Spain.

Table of contents

Experimental Section

General Procedures and Techniques

All manipulations of air and water sensitive compounds were carried out under dry nitrogen using a Braun Labmaster glovebox or standard Schlenk line techniques. ^{1}H and ^{13}C NMR spectra were recorded on a Bruker Ascend TM-500/400 and referenced to the residual deuterated solvent. Thermogravimetric analysis of the products was performed on a TGA instrument (model TGA-Q50). The heating rate for the sample was 10 °C/min and the nitrogen flow rate was 60 mL/min. Differential scanning calorimetry (DSC) curves were obtained under a N_2 atmosphere on TA Instrument (model DSC-Q20). Samples were weighed into aluminum crucibles with 5 mg of sample and subjected to two heating cycles at a heating rate of 10 °C/min. Gel permeation chromatography (GPC) measurements were performed on a Polymer Laboratories PL-GPC-220 instrument equipped with a TSK-GEL G3000H column and an ELSD-LTII light scattering detector or/and a RID-20A differential Refractive Index Detector. The GPC column was eluted with THF at 50 °C at a flow rate of 1 mL min^{-1} and was calibrated using eight monodisperse polystyrene standards in the range 580–48300 Da.

Materials and reagents

Solvents were pre-dried over sodium wire (THF) or $CaCl_2$ (DCM) and distilled under nitrogen from sodium (toluene, THF) or $CaCl_2$ (DCM). Deuterated solvents were stored over activated 4 Å molecular sieves and degassed by several freeze thaw cycles. $InCl_3$ (Sigma-Aldrich) was kept in the glovebox and used as received. Cyclohexene oxide (Sigma-Aldrich) was pre-dried over calcium hydride, distilled under vacuum and stored under nitrogen in a glove box. *L*-lactide (Sigma-Aldrich) was sublimed three times prior

to use. All other reagents were purchased from common commercial sources and used as received.

Synthesis of $[InCl_2\{(\kappa^3\text{-bpzbe})(\mu\text{-O})\}]_2$ **1.**

In a 100 mL Schlenk tube, bpzbeH (1.00 g, 3.45 mmol) was dissolved in 30 mL of dry THF and cooled down to −78 ºC. Then, a solution of ^{n}BuLi (1.6M in hexanes, 2.30 mL, 3.62 mmol) was added dropwise and the mixture was maintained at −78 ºC for one hour. After that time, the lithiated adduct was transferred *via* cannula to a pre-cooled slurry of $InCl_3$ (0.80 g, 3.62 mmol) in THF. The resulting mixture was warmed to room temperature and left stirring overnight. The white solid precipitated was filtered and dried *in vacuo* for two hours to afford complex **1** in 80% yield. Suitable crystals for X-Ray analysis were obtained from a CH_2Cl_2 solution at room temperature. ^{1}H-NMR (500MHz, CD_3CN, 298 K): δ = 6.18 (d, J_{HH} = 2.4 Hz, 1H, *CH*), 5.98 (s, 1H, $H^{4,4'}$), 5.92 (s, 1H, $H^{4,4'}$), 3.78 (d, J_{HH} = 2.3 Hz, 1H, C^aH), 2.45, 2.41 (s, 6H, $Me^{3,3'}$), 2.32 (brs, 6H, $Me^{5,5'}$), 0.68 (s, 9H, ^tBu). ^{13}C-{^{1}H}-NMR (125MHz, CD_3CN, 298 K): 151.3, 150.5, 141.4, 139.4 ($C^{3,3'}$, $C^{5,5'}$), 107.8, 106.6 ($C^{4,4'}$), 86.0 (C^a), 64.4 (*CH*), 36.3 (*C*-^{t}Bu), 26.1 (^tBu), 13.6 ($Me^{3,3'}$), 11.7, 11.1 ($Me^{5,5'}$). Anal. Calcd. (%) for $C_{32}H_{50}Cl_2In_2N_8O_2$: C, 43.7; H, 5.7; N, 12.7; Found: C, 43.9; H, 5.8; N, 12.5.

Synthesis of $[InCl_2\{(\kappa^3\text{-bpzte})(\mu\text{-O})\}]_2$ **2**.

The synthesis of complex **2** was carried out following the same experimental procedure as complex **1**, using bpzteH (1.00 g, 3.10 mmol), ^{n}BuLi (2.00 mL, 3.24 mmol) and $InCl_3$ (0.72 g, 3.24 mmol). Complex **2** was obtained as a white solid in 70% yield. ^{1}H-NMR (500MHz, CD_2Cl_2, 298 K): δ = 7.25 (d, J_{HH} = 8.0 Hz, 2H, ^oHPh), 7.12 (d, J_{HH} = 7.8 Hz, 2H, ^mHPh), 6.07 (brs, 1H, *CH*), 6.01 (brs, C^aH), 5.98 (s, 1H, $H^{4,4'}$), 5.71 (s, 1H $H^{4,4'}$), 2.56, 1.95 (s, 6H, $Me^{3,3'}$), 2.45, 1.63 (s, 6H, $Me^{5,5'}$), 2.36 (s, 3H, *Me*Ph). ^{13}C-{^{1}H}-NMR (125MHz, CD_2Cl_2, 298 K): 152.1-137.4 ($C^{3,3'}$, $C^{5,5'}$), 141.6-139.8 ($C^{ipso\text{-}p}$-Ph), 128.8 (C^m-Ph), 126.9 (C^o-Ph), 107.0, 106.2 ($C^{4,4'}$), 79.2 (C^a), 67.7 (*CH*), 20.9 (*Me*-Ph), 13.9, 13.3 ($Me^{3,3'}$), 10.9, 9.9 ($Me^{5,5'}$). Anal. Calcd. (%) for $C_{38}H_{46}Cl_2In_2N_8O_2$: C, 48.2; H, 4.9; N, 11.8; Found: C, 48.5; H, 5.1; N, 11.6.

Synthesis of $[InCl_2\{(\kappa^3\text{-bpzappe})(\mu\text{-O})\}]_2$ **3**.

The synthesis of complex **3** was carried out following the same experimental procedure as complex **1**, using bpzappeH (1.00 g, 2.33 mmol), ^{n}BuLi (1.53 mL, 2.44 mmol) and $InCl_3$ (0.54 g, 2.44 mmol). Complex **3** was obtained as a white solid in 70% yield. ^{1}H-NMR (500MHz, CD_3CN, 298 K): δ = 7.68 (d, J_{HH} = 7.3 Hz, 2H, ^{o}*H*Ph), 7.24 (m, 5H, *Ph*), 6.59 (d, J_{HH} = 8.4 Hz, 2H, ^{m}*H*Ph), 6.53 (s, 1H, *CH*), 5.88 (s, 1H, $H^{4,4'}$), 5.76 (s, 1H, $H^{4,4'}$), 2.89 (s, 6H, NMe_2), 2.55, 2.50 (s, 6H, $Me^{3,3'}$), 2.10, 2.08 (s, 6H, $Me^{5,5'}$). ^{13}C-{^{1}H}-NMR (125MHz, CD_3CN, 298 K): 150.0-141.2 ($C^{3,3'}$, $C^{5,5'}$), 149.7-126.7 (*Ph*), 127.7 (C^{m}-NPh), 111.2 (C^{o}-NPh), 106.0, 105.9 ($C^{4,4'}$), 85.0 (C^{a}), 69.5 (*CH*), 39.6 (NMe_2), 13.2, 13.1 ($Me^{3,3'}$), 10.4 ($Me^{5,5'}$). Anal. Calcd. (%) for $C_{52}H_{60}Cl_2In_2N_{10}O_2$: C, 54.0; H, 5.2; N, 12.1; Found: C, 54.3; H, 5.3; N, 11.8.

Synthesis of $[InCl_2\{(\kappa^3\text{-bpzFerr})(\mu\text{-O})\}]_2$ **4**.

The synthesis of complex **4** was carried out following the same experimental procedure as complex **1**, using bpzFerrH (1.00 g, 2.40 mmol), ^{n}BuLi (1.57 mL, 2.51 mmol) and $InCl_3$ (0.56 g, 2.51 mmol). Complex **4** was obtained as an orange solid in 76% yield. ^{1}H-NMR (500MHz, CD_3CN, 298 K): δ = 6.07 (s, 1H, $H^{4,4'}$), 6.03 (d, J_{HH} = 3.4 Hz, 1H, C*H*), 5.75 (s, 1H, $H^{4,4'}$), 5.34 (d, J_{HH} = 3.2 Hz, 1H, $C^{a}H$), 4.63-3.89 (s, 4H, Cp), 4.18 (s, 5H, Cp'), 2.56, 2.48 (s, 6H, $Me^{3,3'}$), 2.48, 2.05 (s, 6H, $Me^{5,5'}$). ^{13}C-{^{1}H}-NMR (125MHz, CD_3CN, 298 K): 150.2-140.0 ($C^{3,3'}$, $C^{5,5'}$), 106.2, 105.8 ($C^{4,4'}$), 91.3 (C_p), 76.4 (s, 1H, C^{a}), 68.5-64.1(*Cp, Cp'*), 68.0 (*CH*), 13.1, 13.0 ($Me^{3,3'}$), 10.1 ($Me^{5,5'}$). Anal. Calcd. (%) for $C_{44}H_{50}Cl_2Fe_2In_2N_8O_2$: C, 46.6; H, 4.4; N, 9.9; Found: C, 46.9; H, 4.7; N, 9.8.

Figure S1. ^{1}H-NMR spectrum of [$InCl_2${(κ^3-bpzbe)(μ-O)}]$_2$ **1** in CD_3CN.

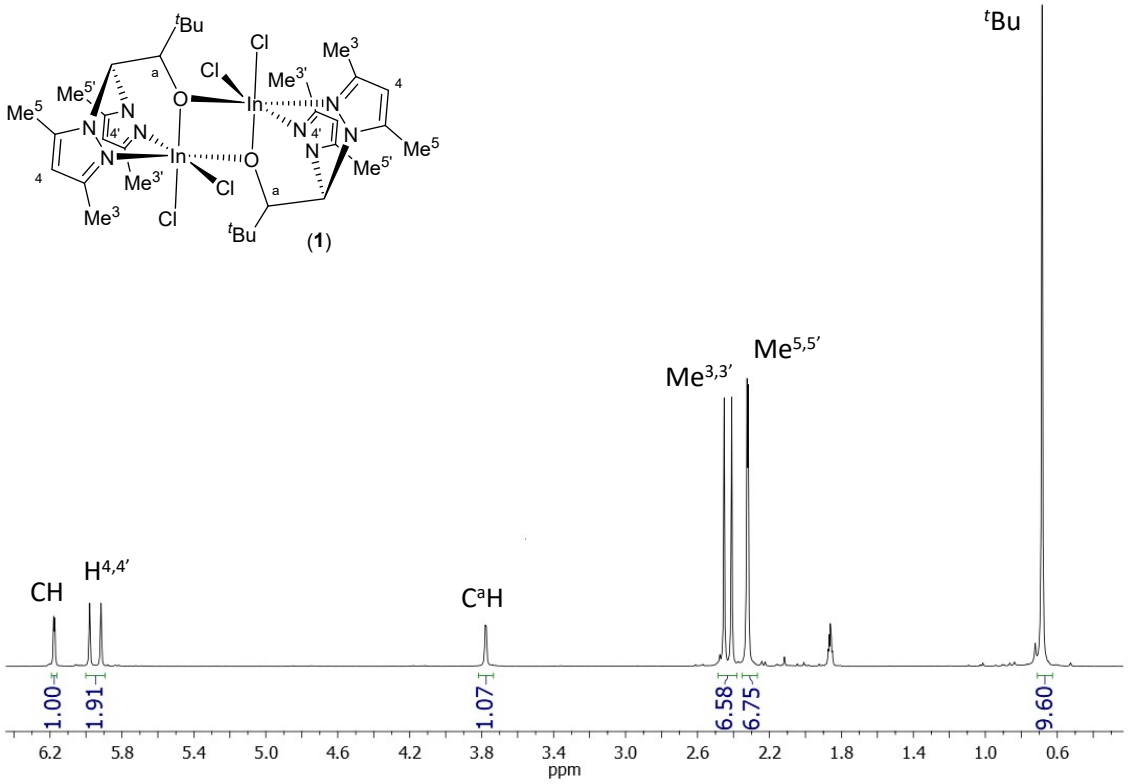

Figure S2. ^{13}C-{^{1}H}-NMR spectrum of [$InCl_2${(κ^3-bpzbe)(μ-O)}]$_2$ **1** in CD_3CN.

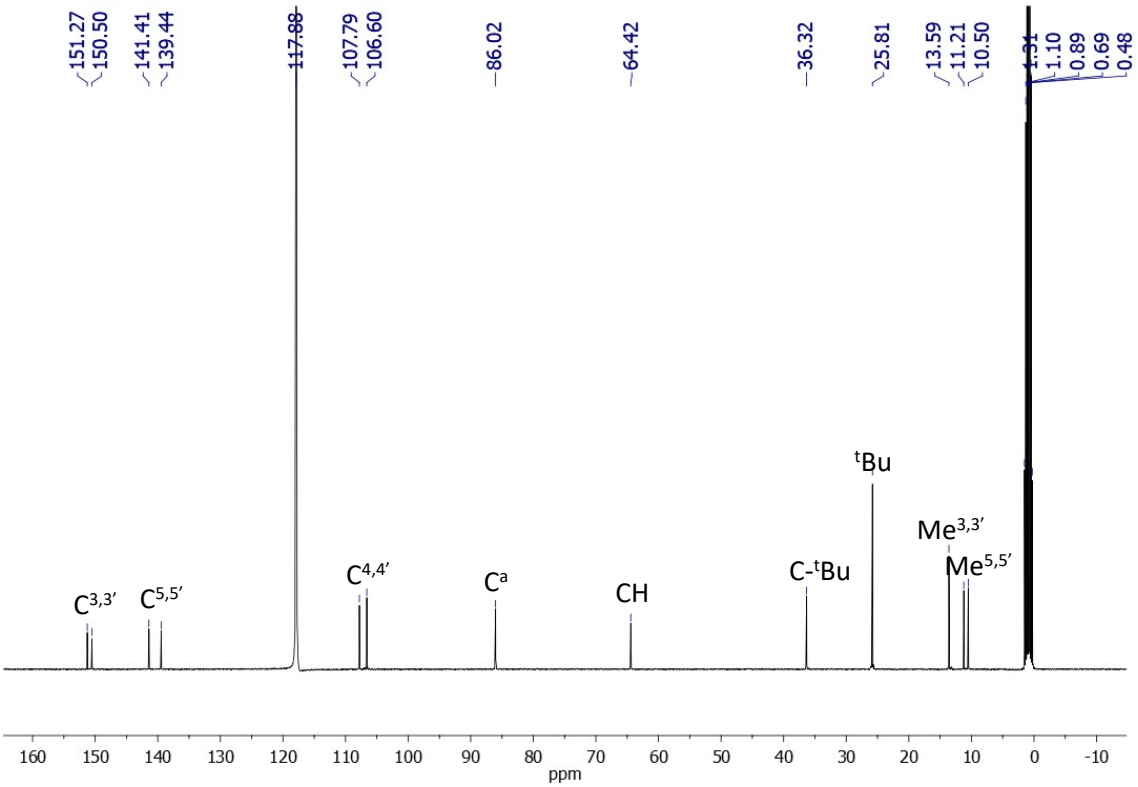

Figure S3. ^{1}H-NMR spectrum of $[InCl_2\{(\kappa^3\text{-bpzte})(\mu\text{-O})\}]_2$ **2** in CD_2Cl_2.

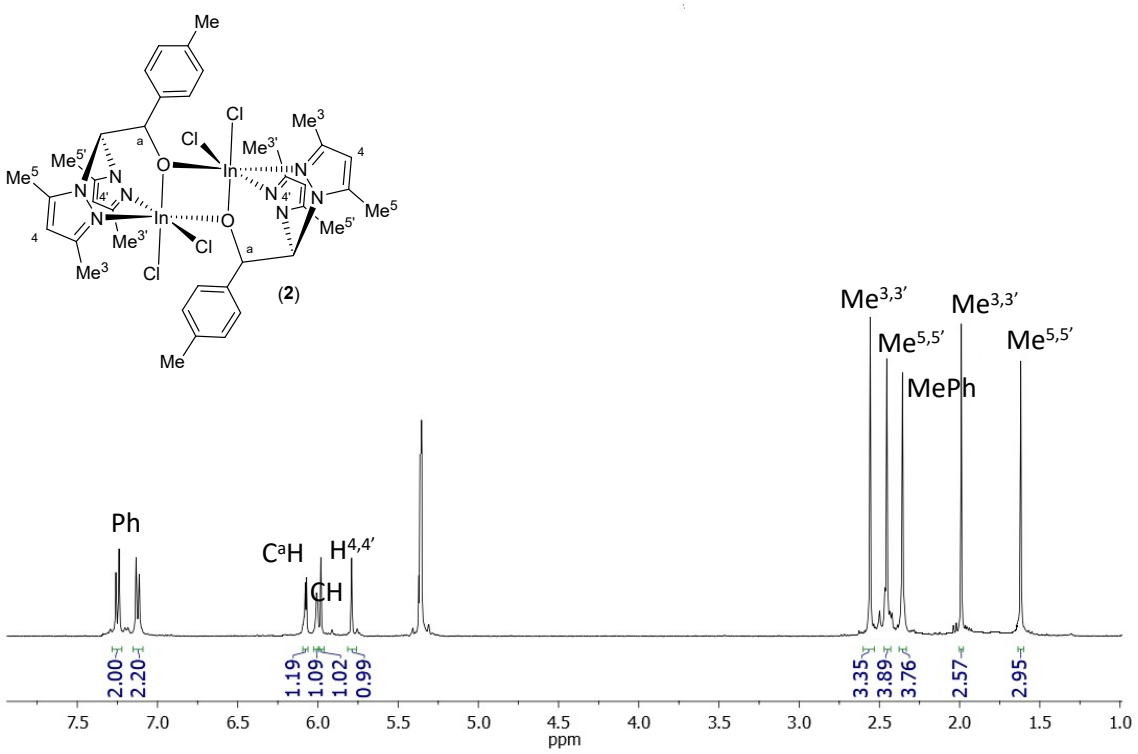

Figure S4. ^{13}C-{^{1}H}-NMR spectrum of $[InCl_2\{(\kappa^3\text{-bpzte})(\mu\text{-O})\}]_2$ **2** in CD_2Cl_2.

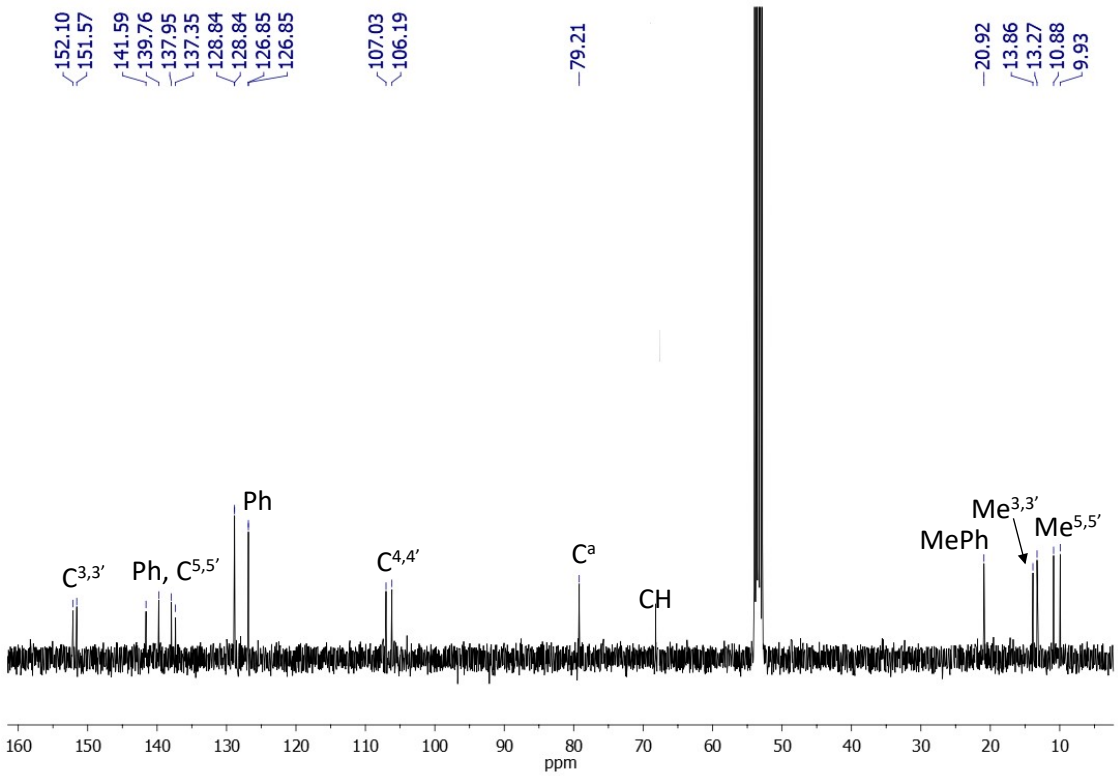

Figure S5. ^{1}H-NMR spectrum of [$InCl_2${(κ^3-bpzappe)(μ-O)}]$_2$ **3** in CD_3CN.

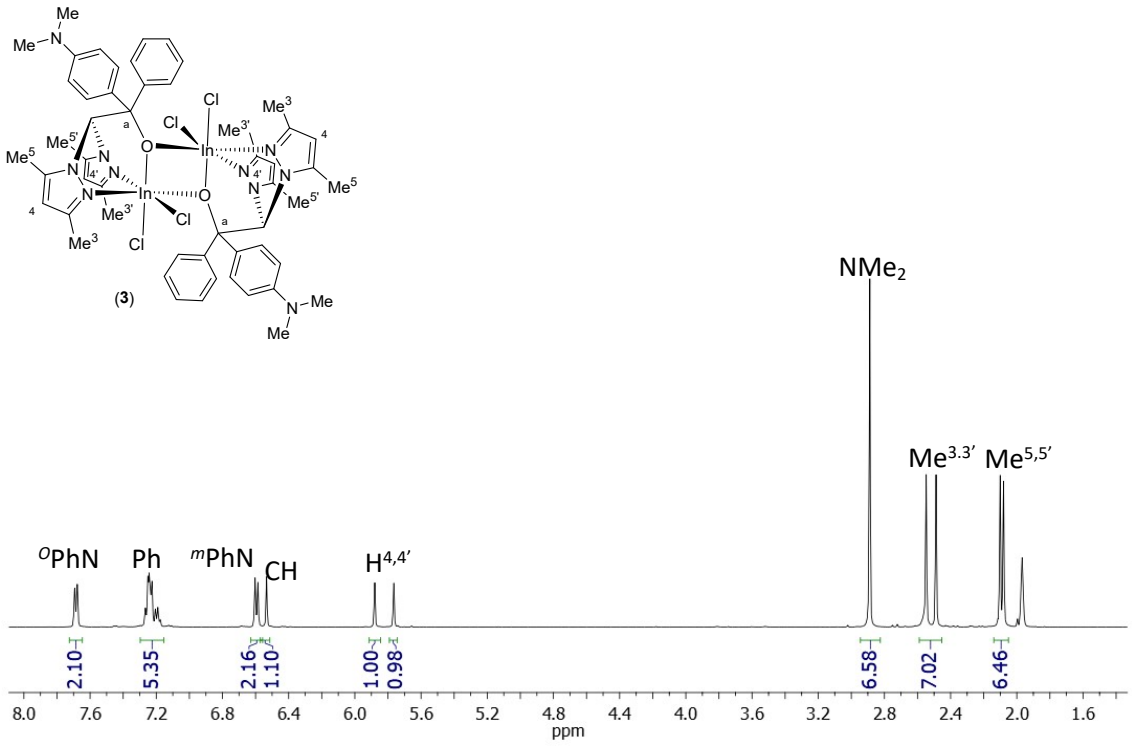

Figure S6. ^{13}C-{^{1}H}-NMR spectrum of [$InCl_2${(κ^3-bpzappe)(μ-O)}]$_2$ **3** in CD_3CN.

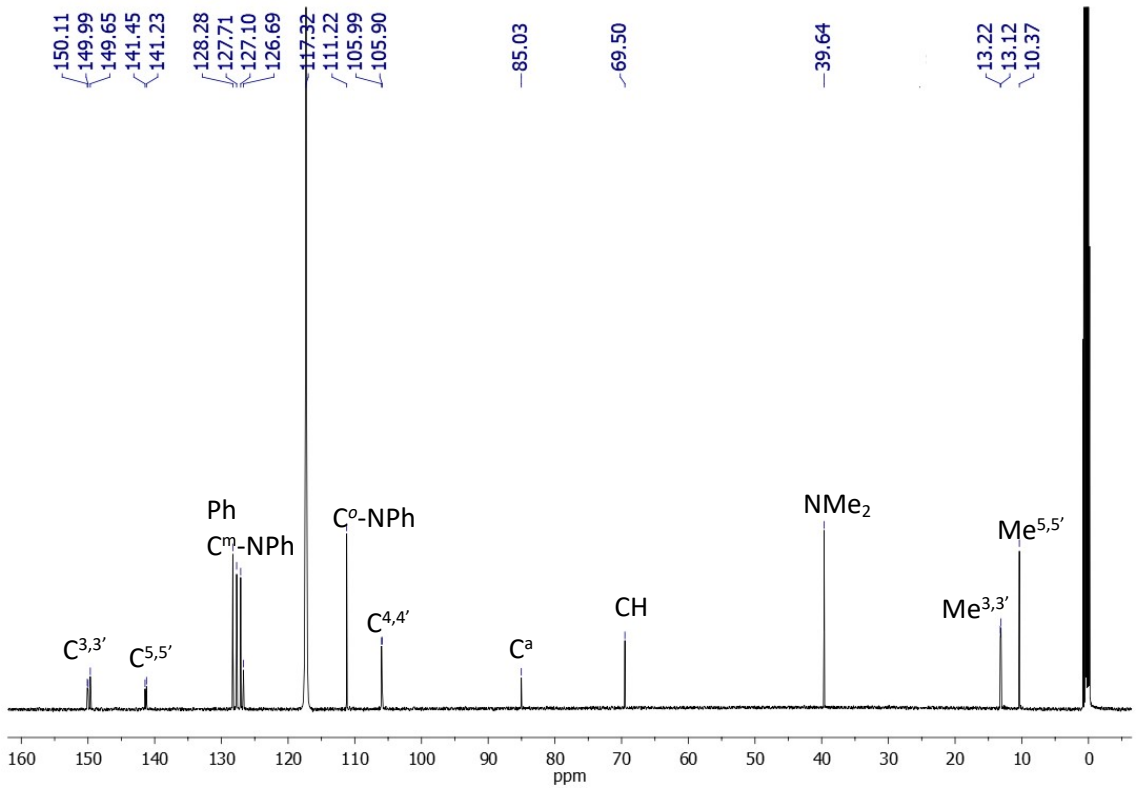

Figure S7. ^{1}H-NMR spectrum of $[InCl_2\{(\kappa^3\text{-bpzFerr})(\mu\text{-O})\}]_2$ **4** in CD_3CN.

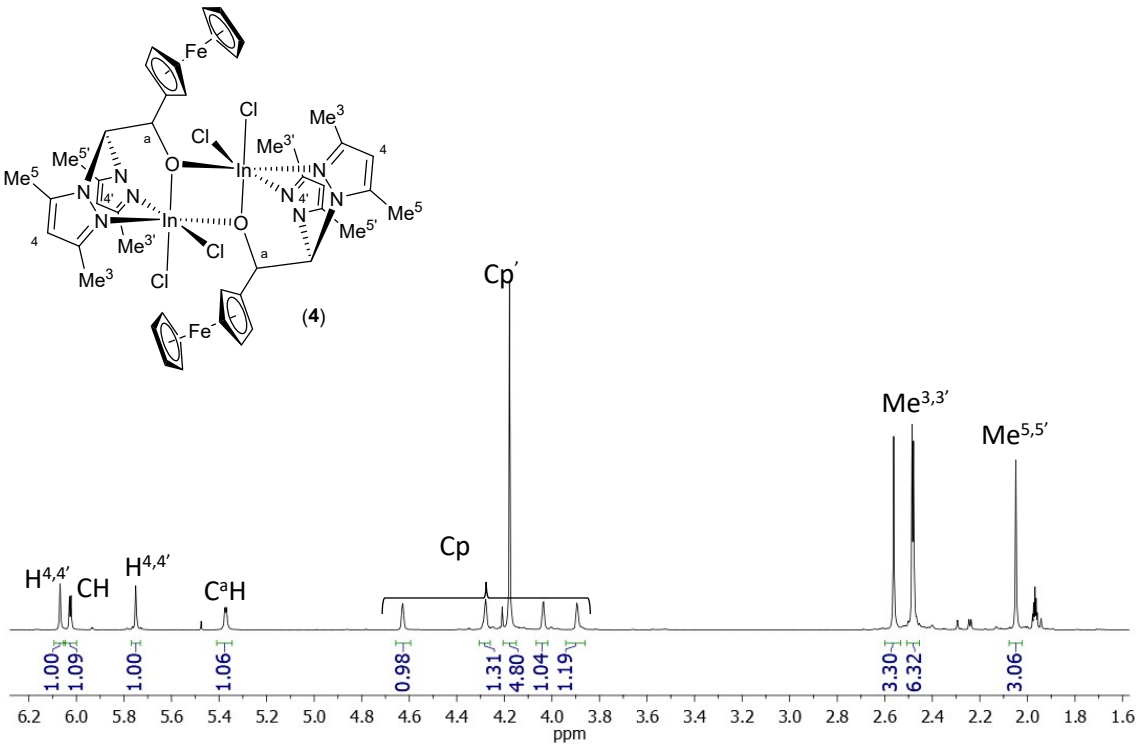

Figure S8. ^{13}C-{^{1}H}-NMR spectrum of $[InCl_2\{(\kappa^3\text{-bpzFerr})(\mu\text{-O})\}]_2$ **4** in CD_3CN.

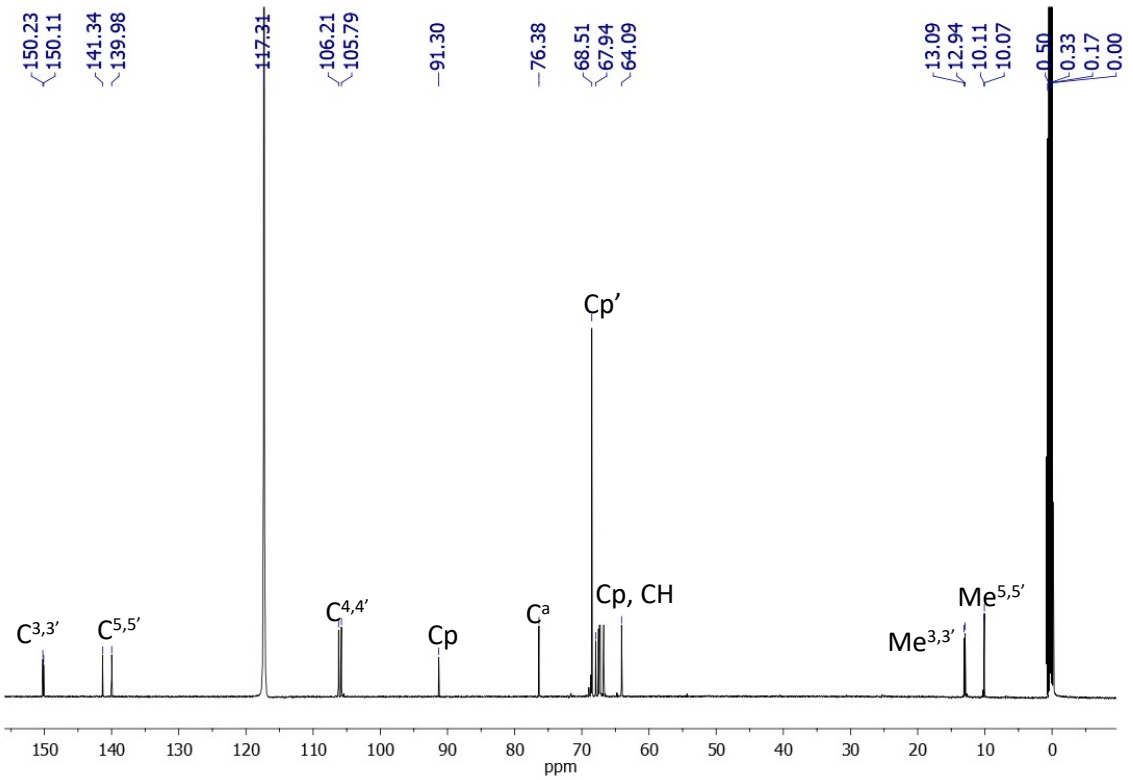

X-ray Crystallographic Structure Determination

Data collection and refinement parameters for **1xCHCl$_3$** and selected bond lengths and angles are given in Tables S1 and S2. CCDC Numbers 2168127. A single crystal of **1xCHCl$_3$** was coated with high-vacuum grease, mounted on a glass fiber, and transferred to a Bruker APEX II CCD-based diffractometer equipped with a graphite-monochromated MoKα radiation source (λ=0.71073 Å). The highly redundant datasets were integrated with SAINT and corrected for Lorentzian and polarization effects. A semi-empirical absorption correction was applied to the diffraction data using SADABS. The software package OLEX2 was used for structure solution and refinement by full-matrix least-squares methods based on F^2. A successful solution by direct methods provided most non-hydrogen atoms from the E map. The remaining non-hydrogen atoms were located in an alternating series of least-squares cycles and difference Fourier maps. The non-hydrogen atoms were refined with anisotropic displacement coefficients and hydrogen atoms were placed by using a riding model and included in the refinement at calculated positions.

	1xCHCl$_3$
Empirical formula	C_{34} H_{54} Cl_8 In_2 N_8 O_2
Formula weight	1120.09
Temperature	245(2)
Wavelength	0.71073
Crystal system	Orthorhombic
Space group	P c c n
a (Å)	14.946(4)
b (Å)	15.760(4)
c (Å)	19.285(5)
α (º)	90
β (º)	90
γ (º)	90
Volume (Å^3)	4542.7(19)
Z	4
Density (calculated) (mg/m^3)	1.638
Absorption coefficient (mm^{-1})	1.526
F(000)	2256
Crystal size (mm^3)	0.18 x 0.11 x 0.08
Index ranges	$-18 \leq h \leq 18$, $-19 \leq k \leq 18$, $-24 \leq l \leq 24$
Independent reflections	4651 [R(int) = 0.0724]
Data / restraints / parameters	4651 / 0 / 251
Goodness-of-fit on F^2	1.055
Final R indices [I>2σ(I)]	R1 = 0.0535, wR2 = 0.1275
R indices (all data)	R1 = 0.0758, wR2 = 0.1405
Largest diff. peak and hole, e.Å^{-3}	1.060 and -1.316

Table S1. Crystallographic data for complex **1xCHCl$_3$**.

Table S2. Distances and angles for complex**1xCHCl$_3$**.

1xCHCl$_3$ (Bond distances, Å)		**1xCHCl$_3$** (Bond Angles, º)	
In(1)–O(1)	2.156(4)	O(1)–In(1)–O(1A)	76.7(1)
In(1)–O(1A)	2.171(4)	O(1)–In(1)–N(1)	85.9(1)
In(1)–N(1)	2.267(5)	O(1A)–In(1)–N(1)	162.2(1)
In(1)–N(3)	2.371(4)	O(1)–In(1)–N(3)	78.1(1)
In(1)–Cl(1)	2.407(2)	O(1A)–In(1)–N(3)	96.1(1)
In(1)–Cl(2)	2.415(1)	N(1)–In(1)–N(3)	76.3(1)
N(1)–C(3)	1.332(7)	O(1)–In(1)–Cl(1)	165.8(1)
N(1)–N(2)	1.355(7)	O(1A)–In(1)–Cl(1)	98.0(1)
N(2)–C(1)	1.353(7)	N(1)–In(1)–Cl(1)	98.0(1)
N(2)–C(11)	1.433(7)	N(3)–In(1)–Cl(1)	89.5(1)
N(3)–C(8)	1.326(7)	O(1)–In(1)–Cl(2)	95.6(1)
N(3)–N(4)	1.368(6)	O(1A)–In(1)–Cl(2)	94.90(9)
N(4)–C(6)	1.369(6)	N(1)–In(1)–Cl(2)	90.5(1)
N(4)–C(11)	1.451(6)	N(3)–In(1)–Cl(2)	165.7(1)
O(1)–C(12)	1.410(6)	Cl(1)–In(1)–Cl(2)	97.92(5)
C(1)–C(2)	1.367(9)	C(3)–N(1)–N(2)	106.8(5)
C(1)–C(4)	1.476(9)	C(3)–N(1)–In(1)	134.1(4)
C(2)–C(3)	1.400(9)	N(2)–N(1)–In(1)	118.7(3)
C(3)–C(5)	1.458(8)	C(1)–N(2)–N(1)	111.3(5)
C(6)–C(7)	1.364(8)	C(1)–N(2)–C(11)	128.5(5)
C(6)–C(9)	1.478(8)	N(1)–N(2)–C(11)	120.2(4)
C(7)–C(8)	1.405(8)	C(8)–N(3)–N(4)	106.3(4)
C(8)–C(10)	1.468(8)	C(8)–N(3)–In(1)	138.2(4)
C(11)–C(12)	1.536(7)	N(4)–N(3)–In(1)	115.5(3)
C(12)–C(13)	1.564(8)	C(6)–N(4)–N(3)	110.9(4)
C(13)–C(14)	1.515(8)	C(6)–N(4)–C(11)	127.3(5)
C(13)–C(15)	1.514(8)	N(3)–N(4)–C(11)	119.9(4)
C(13)–C(16)	1.534(8)	C(12)–O(1)–In(1)	124.1(3)
		C(12)–O(1)–In(1A)	127.2(3)
		In(1)–O(1)–In(1A)	103.3(1)

Optimization parameters for polycarbonate PCHC (5) formation

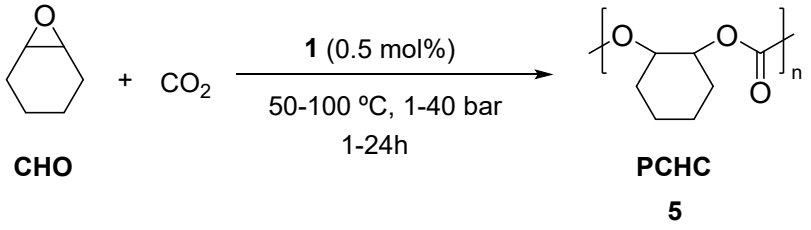

Scheme 1. Optimization of reaction temperature, CO_2 pressure and reaction time for the synthesis of PCHC (**5**) catalyzed by complex **1**.

Table S3. Effect of the reaction temperature on the synthesis of **5** catalyzed by complex **1**.[a]

Entry	Temperature (ºC)	Conv. (%)[b]	Carbonate linkages (%)[b]	Polycarbonate selectivity (%)[b]
1	r.t	0	0	0
2	50	25	>99	>99
3	60	77	>99	>99
4	80	75	>99	>99
5	100	74	>99	95

[a]Reactions carried out 25-100 ºC using 40 bar of CO_2 pressure for 16 hours and employing 0.5 mol% of complex **1**. [b]Conversion, polycarbonate selectivity and PCHC (**5**) content determined by ^{1}H-NMR spectroscopy of the crude reaction mixture.

Table S4. Effect of the reaction pressure on the synthesis of **5** catalyzed by complex **1**.[a]

Entry	Pressure (bar)	Conv. (%)[b]	Carbonate linkages (%)[b]	Polycarbonate selectivity (%)[b]
1	1	47	>99	>99
2	10	53	>99	>99
3	20	61	>99	>99
4	30	73	>99	>99
5	40	77	>99	95

[a]Reactions carried out at 60 ºC using 1-40 bar of CO_2 pressure for 16 hours and employing 0.5 mol% of complex **1**. [b]Conversion, polycarbonate selectivity and PCHC (**5**) content determined by ^{1}H-NMR spectroscopy of the crude reaction mixture.

Figure S9. ^{1}H-NMR spectrum of poly(cyclohexene carbonate) (**5**) in $CDCl_3$.

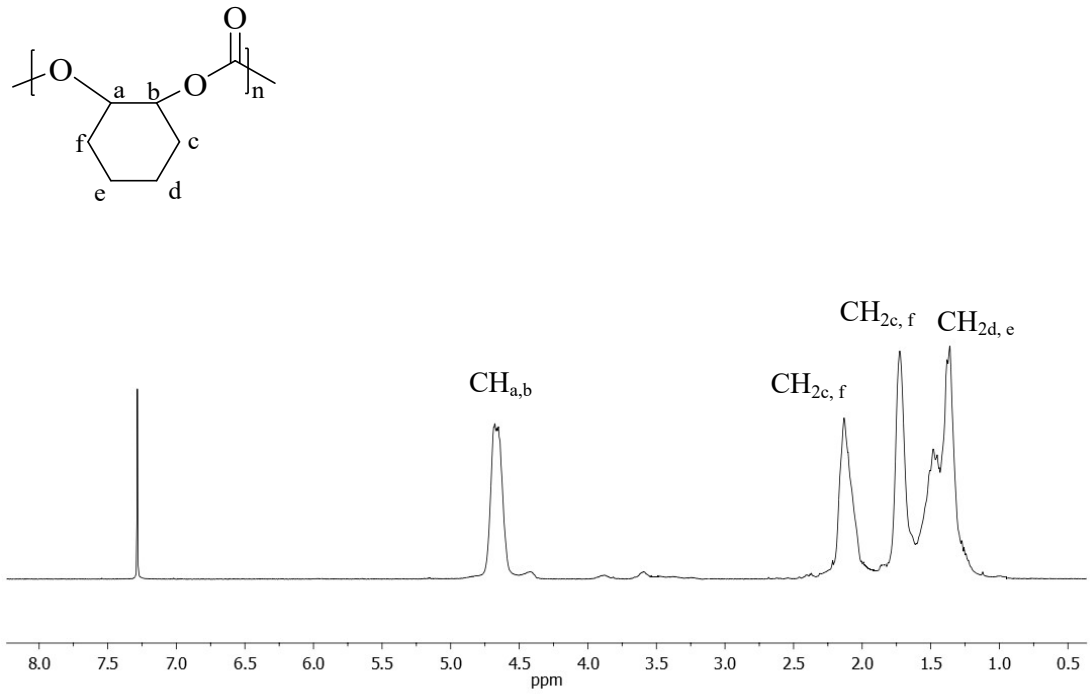

Figure S10. ^{13}C-{^{1}H} NMR spectrum for poly(cyclohexene carbonate) (**5**) in $CDCl_3$.

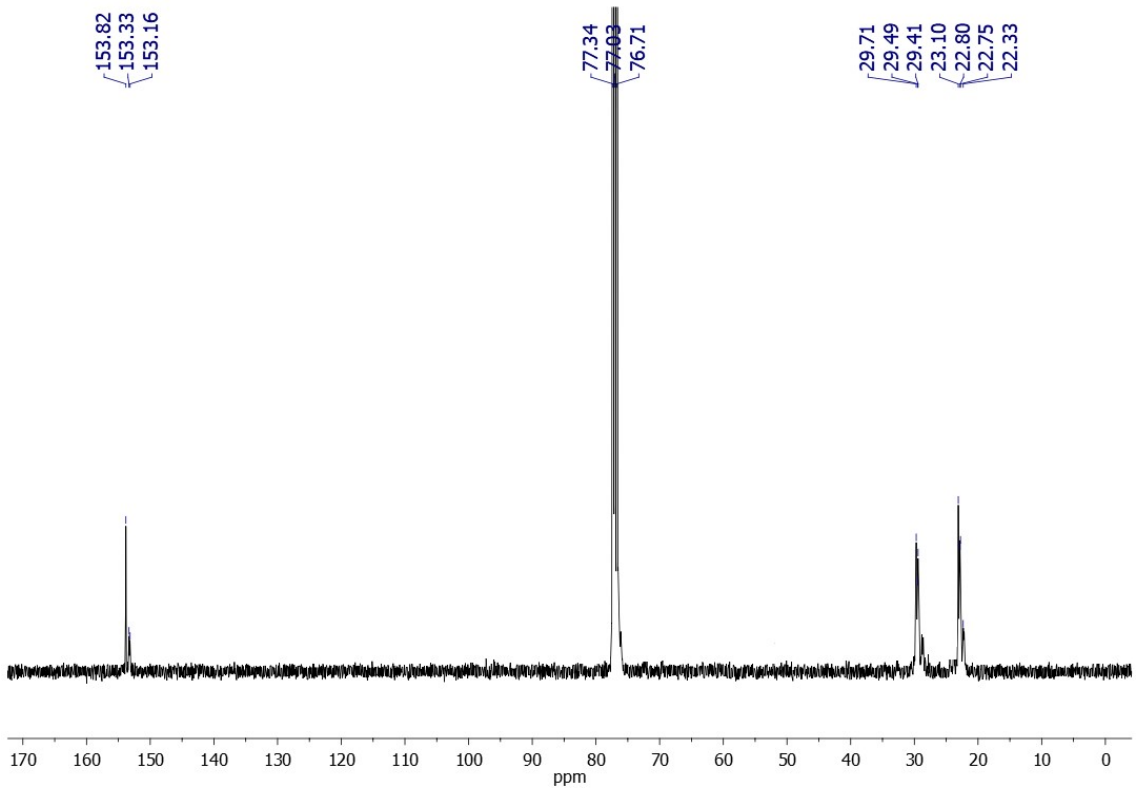

Figure S11. MALDI-TOF spectrum for poly(cyclohexene carbonate) (**5**) in $CDCl_3$.

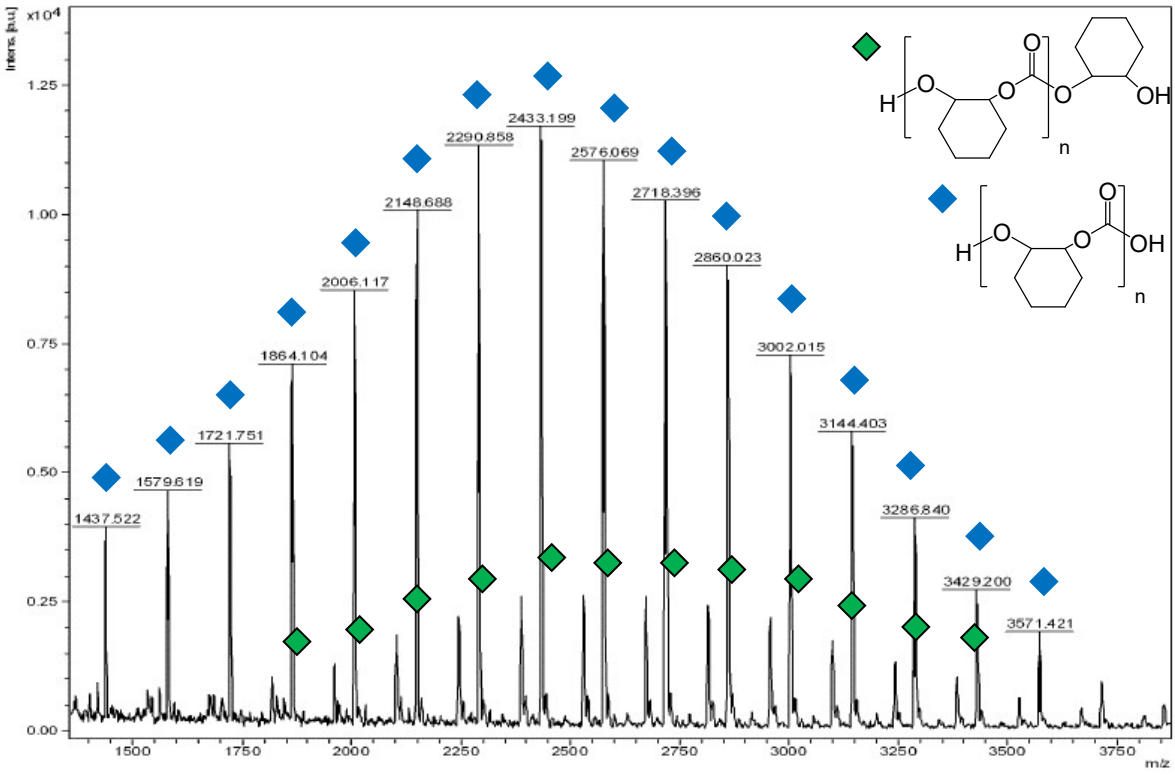

Figure S12. GPC traces for poly(cyclohexene carbonate) (**5**) at one (blue) and 40 bar (red) CO_2 pressure.

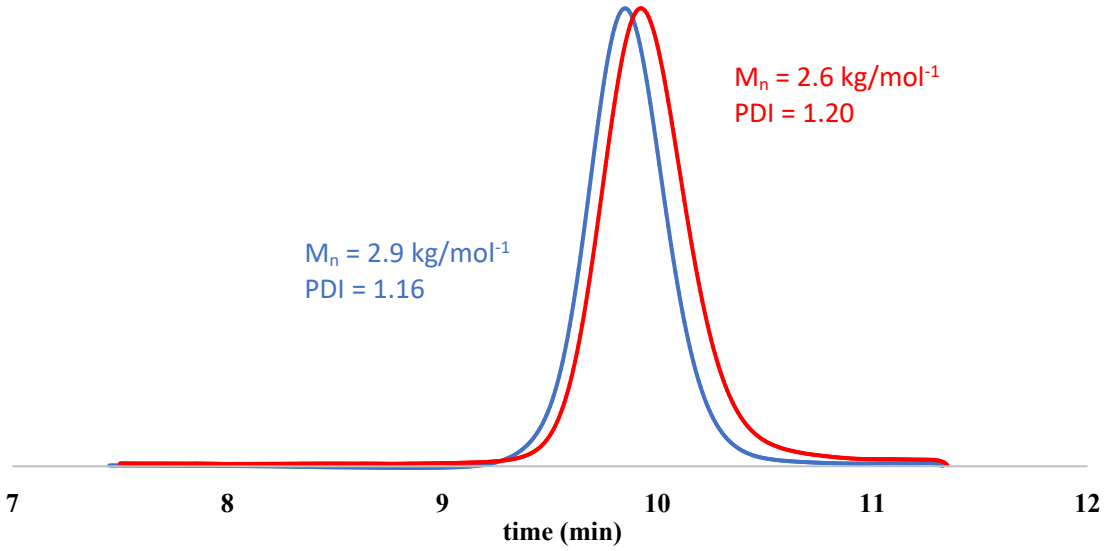

Figure S13. TGA thermogram for poly(cyclohexene carbonate) (**5**).

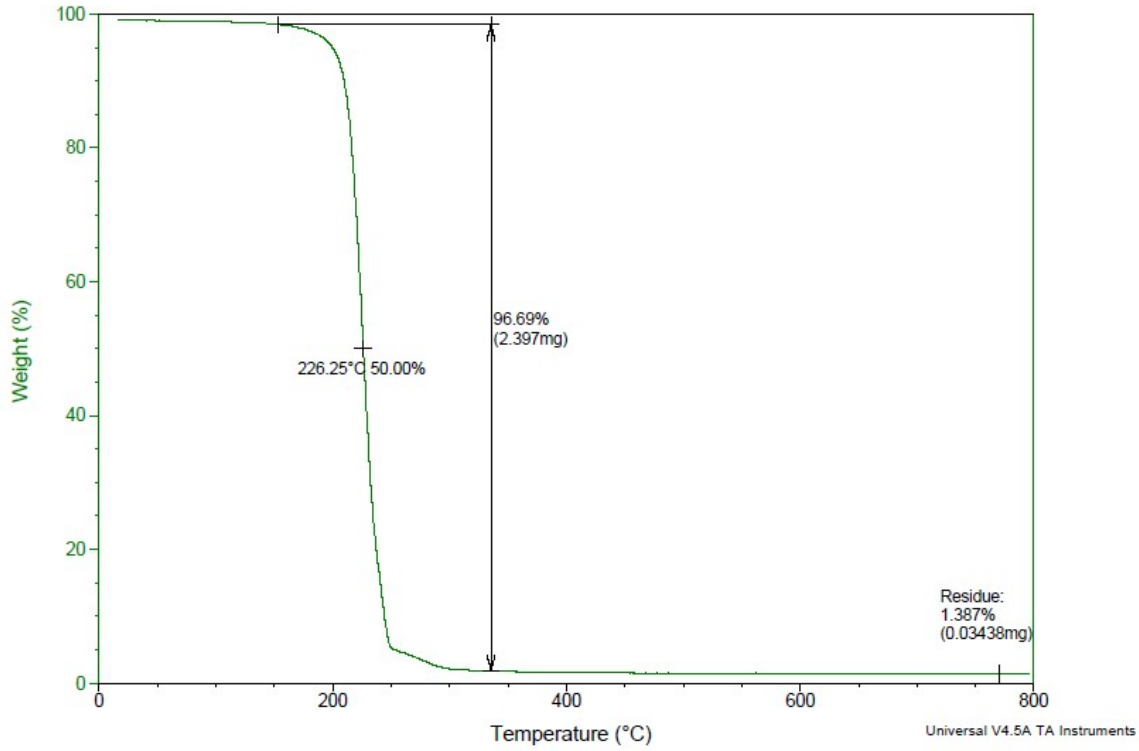

Figure S14. DSC thermogram for poly(cyclohexene carbonate) (**5**).

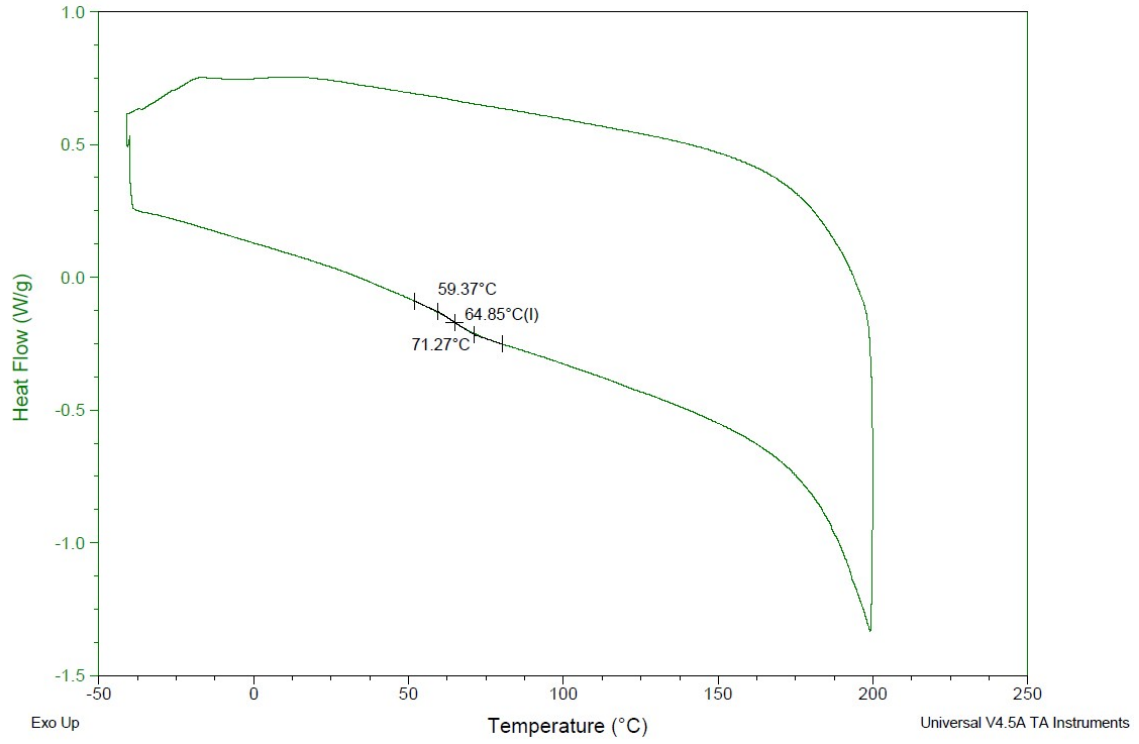

Optimization parameters for terpolymer PLA-PCHC (6) formation

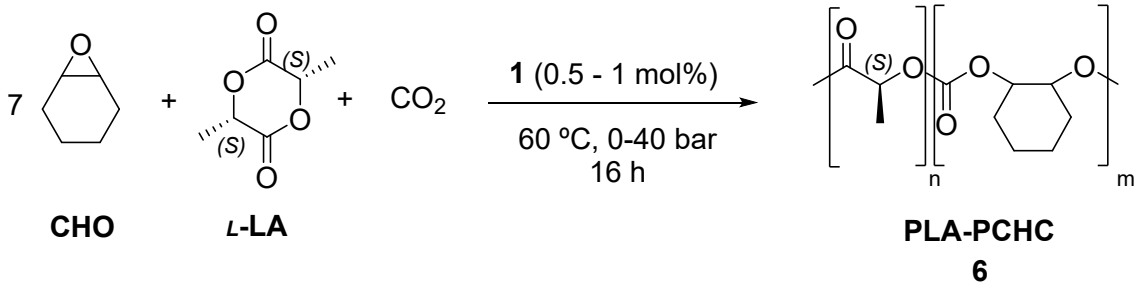

Scheme 2. Optimization of catalyst loading and pressure for the synthesis of terpolymer PLA-PCHC (**6**).

Table S5. Effect of the catalyst loading (**1**) on the synthesis of **6**.[a]

Entry	**1** (mol%)	Conv. (%) CHO [b]	Conv. (%) *L*-LA [b]	PLA(%)[b]	Ether linkages (%)[b]	Carbonate linkages (%)[b]
1	0.5	2.7	100	91	-	9
2	1	17	100	60	-	40

[a]Reactions carried out at 60 ºC using 40 bar of CO_2 pressure for 16 hours. [CHO]:[*L*-LA] = 700:100. [b]Conversions determined by ^{1}H-NMR spectroscopy of the crude reaction mixture.

Table S6. Effect of the pressure on the synthesis of **6** using 0.5 mol% of complex **1**.[a]

Entry	Pressure (bar)	Conv. (%) CHO [b]	Conv. (%) *L*-LA [b]	PLA(%)[b]	Ether linkages (%)[b]	Carbonate linkages (%)[b]
1	1	0	100	100	-	-
2	5	5.5	100	80	-	20
3	10	9	100	78	-	22
4	20	7.5	100	83	-	17
5	30	5.8	100	86	-	14
6	40	2.7	100	90	-	10

[a]Reactions carried out at 60 ºC using 0.5 mol% of complex **1** for 16 hours. [CHO]:[*L*-LA] = 700:100. [b]Conversions determined by ^{1}H-NMR spectroscopy of the crude reaction mixture.

Table S7. Effect of the pressure on the synthesis of **6** using 1 mol% of complex **1**.[a]

Entry	Pressure (bar)	Conv. (%) CHO [b]	Conv. (%) *L*-LA [b]	PLA(%)[b]	Ether linkages (%)[b]	Carbonate linkages (%)[b]
1	1	0	100	100	-	-
2	5	16	100	60	-	40
3	10	27	100	42	-	58
4	20	23	100	48	-	52
5	30	20	100	54	-	46
6	40	17	100	60	-	40

[a]Reactions carried out at 60 ºC using 1 mol% of complex **1** for 16 hours. [CHO]:[*L*-LA] = 700:100. [b]Conversions determined by ^{1}H-NMR spectroscopy of the crude reaction mixture.

Figure S15. Influence of the reaction pressure on the PCHC content in the terpolymer at 0.5 and 1.0 mol% content of complex **1**.

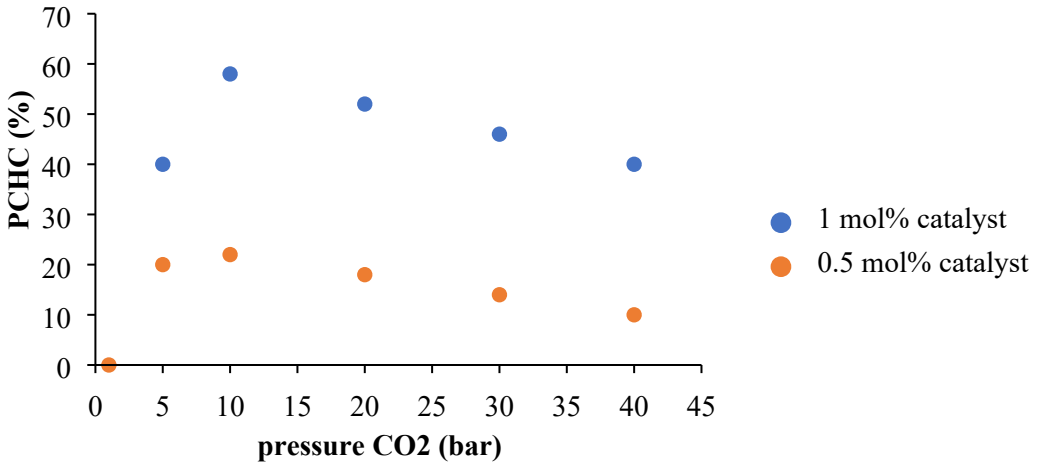

Table S8. Effect of the [CHO]:[*L*-LA] ratio on the synthesis of **6**.[a]

Entry	[CHO]: [*L*-LA]	Conv. (%) CHO [b]	Conv. (%) *L*-LA [b]	PLA(%)[b]	PCHO (%)[b]	PCHC (%)[b]
1	1:1	0	75	100	-	-
2	2:1	18	100	81	-	19
3	3:1	20	100	71	-	29
4	4:1	21	100	64	-	36
5	5:1	24	100	55	-	45
6	7:1	27	100	40	-	60

[a]Reactions carried out at 60 ºC using 1 mol% of complex **1** for 16 hours. [b]Conversions determined by ^{1}H-NMR spectroscopy of the crude reaction mixture.

Figure S16. Plot of % PCHC (**6**) content in **6** vs [CHO]:[*L*-LA] ratio.

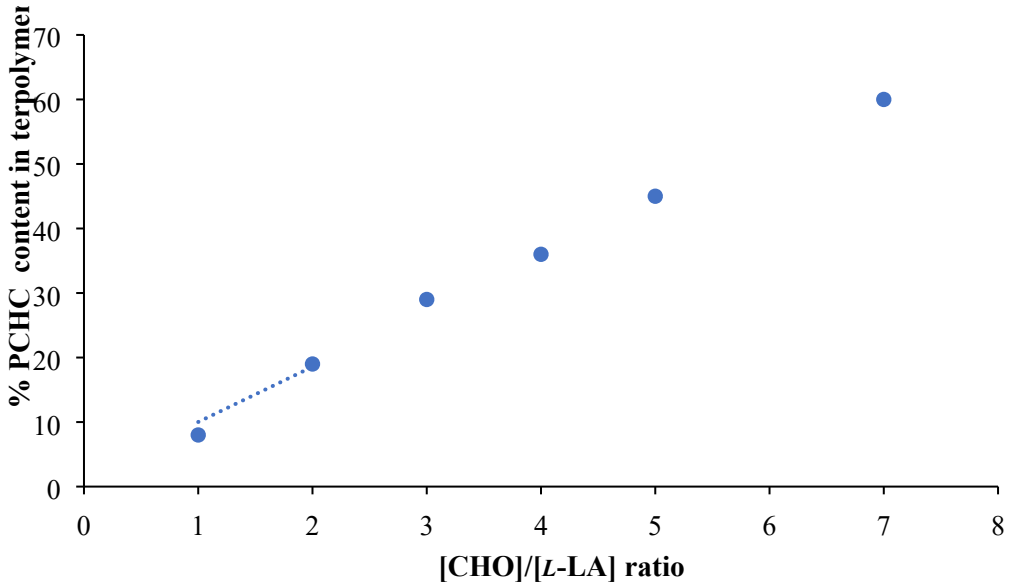

Figure S17. ^{1}H-NMR spectrum of terpolymer **6** in $CDCl_3$.

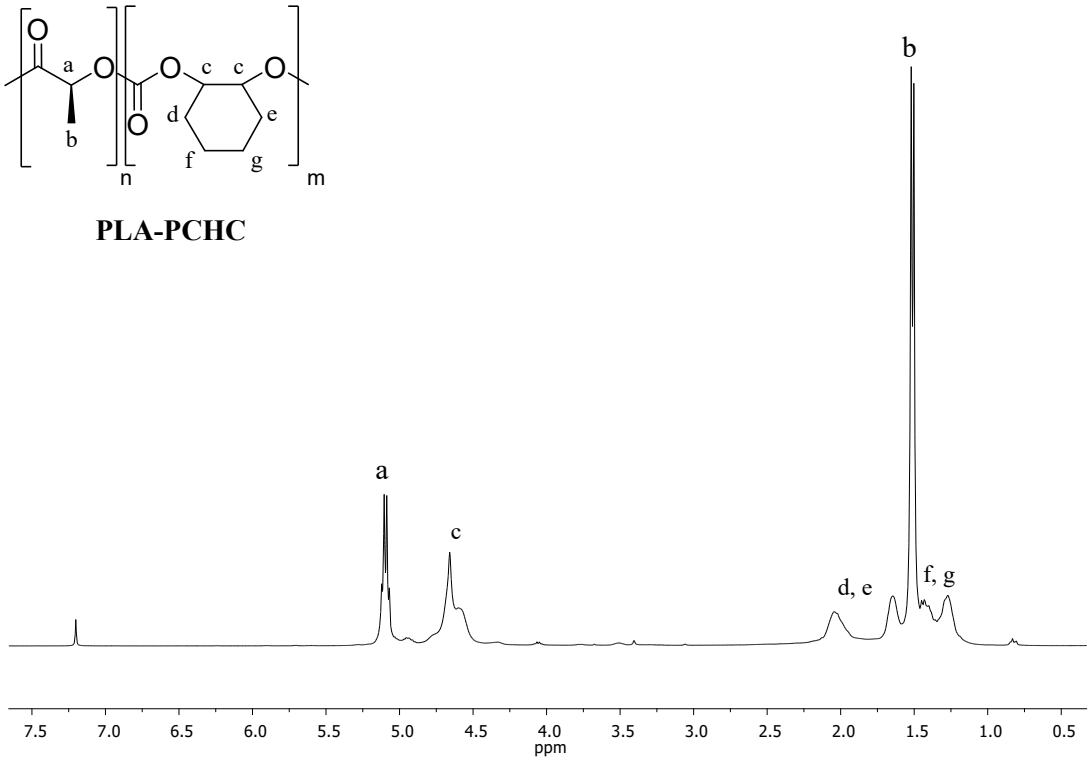

Figure S18. Overlapping NMR spectra of terpolymers synthesized with a [CHO]:[*L*-LA] variable ratio from 1:1 to 7:1.

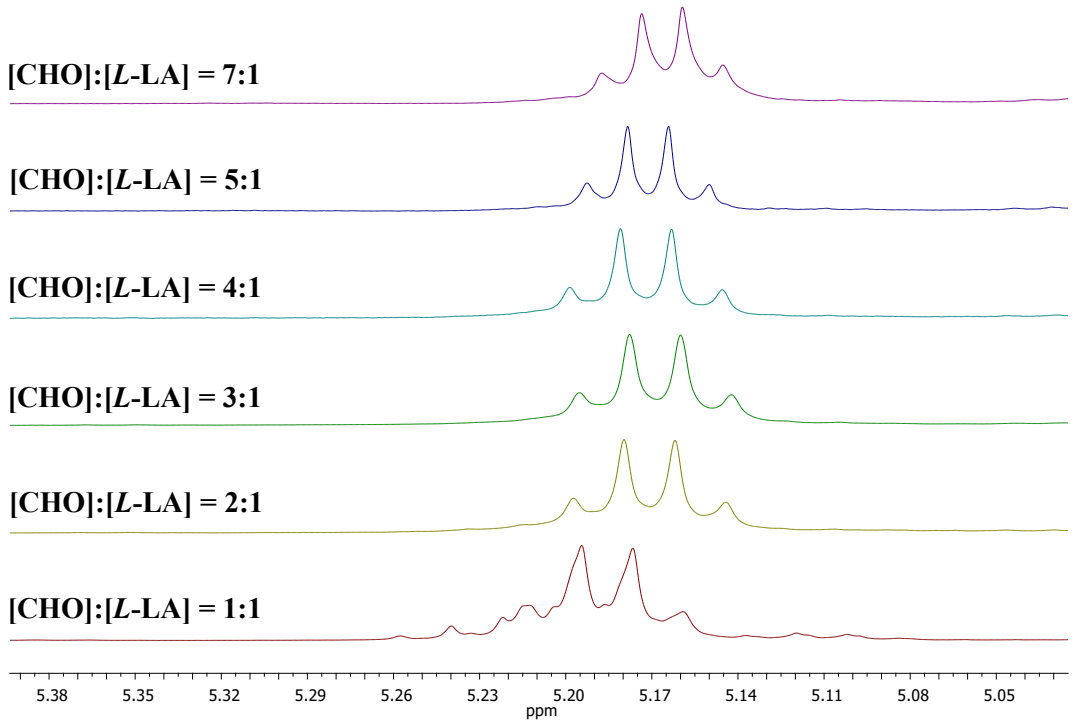

Figure S19. ^{13}C-{^{1}H}-NMR spectrum of terpolymer **6** in $CDCl_3$.

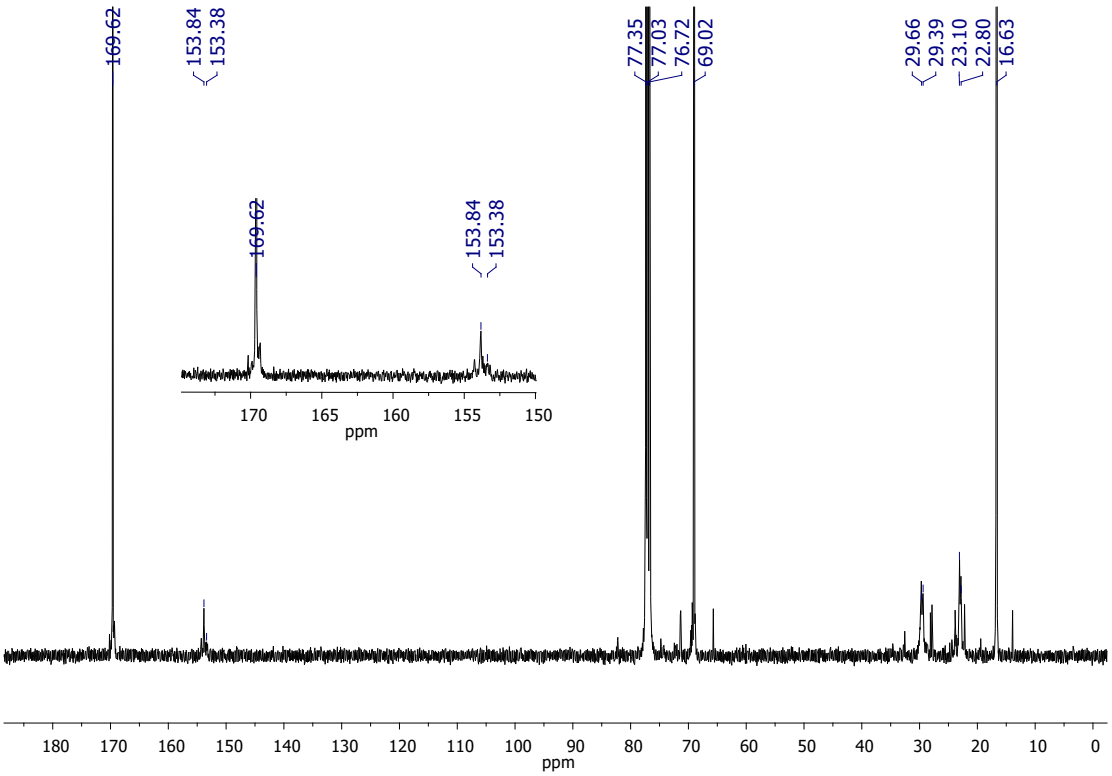

Figure S20. 2D-DOSY-NMR spectrum of terpolymer **6** in $CDCl_3$.

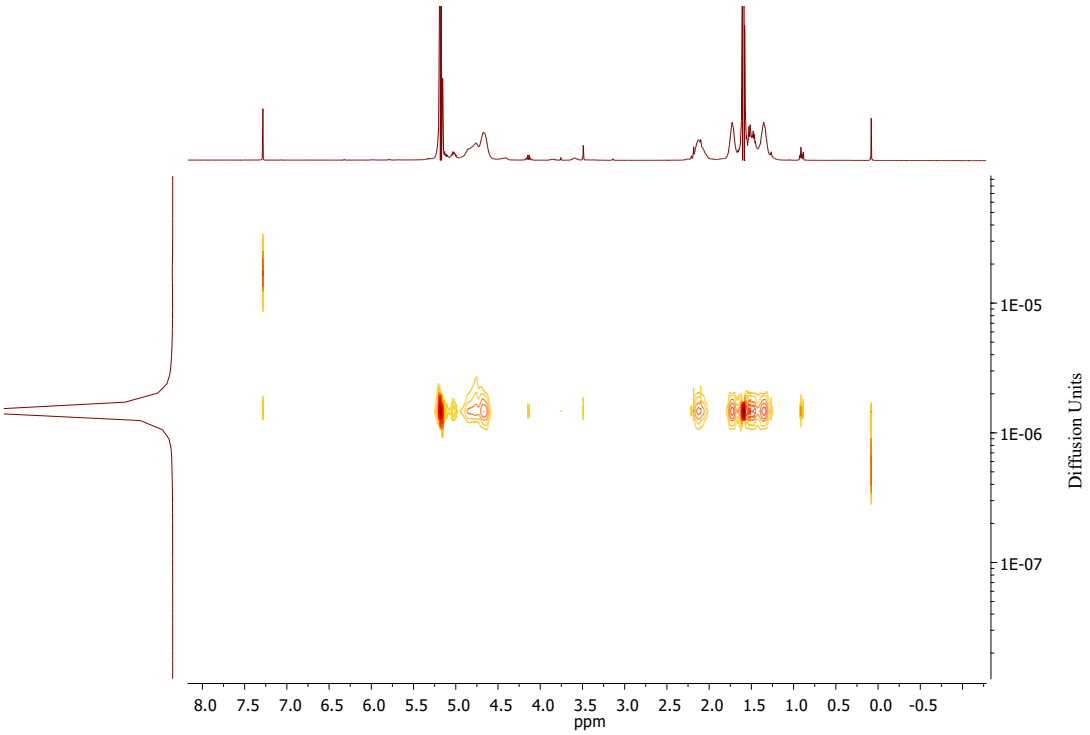

Figure S21. GPC trace for terpolymer **6** at [CHO]:[*L*-LA] 2:1 ratio.

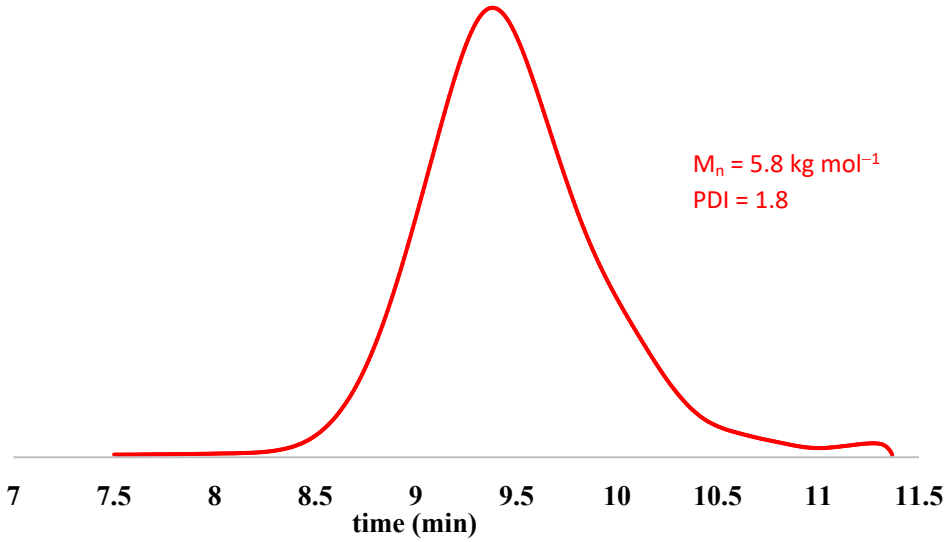

Figure S22. GPC trace for terpolymer **6** at [CHO]:[*L*-LA] 3:1 ratio.

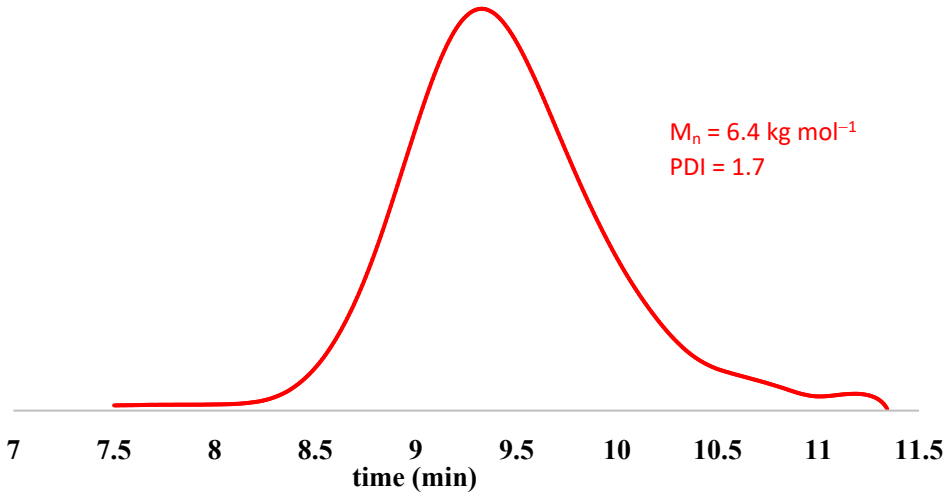

Figure S23. GPC trace for terpolymer **6** at [CHO]:[*L*-LA] 4:1 ratio.

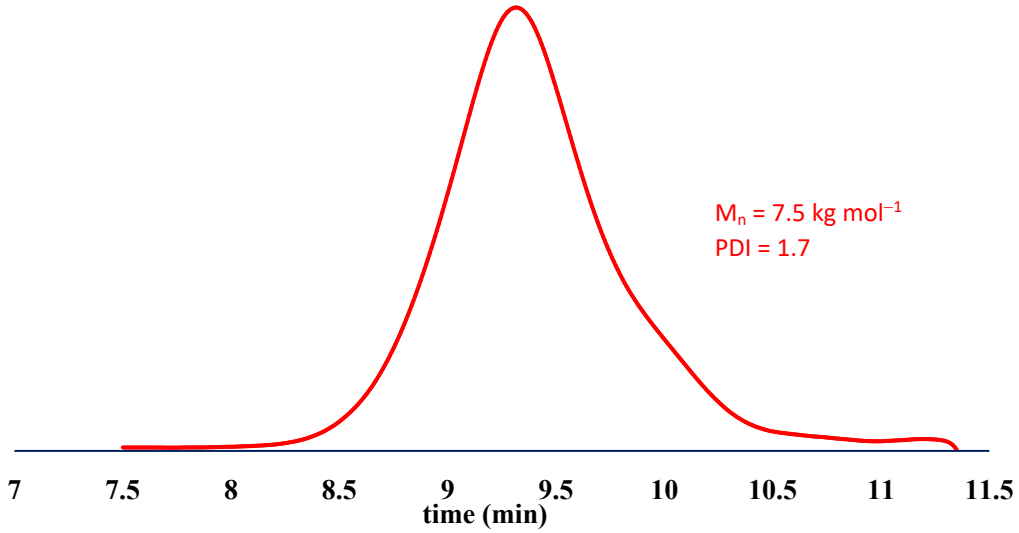

Figure S24. TGA thermogram for terpolymer **6** (Table S8, entry 6).

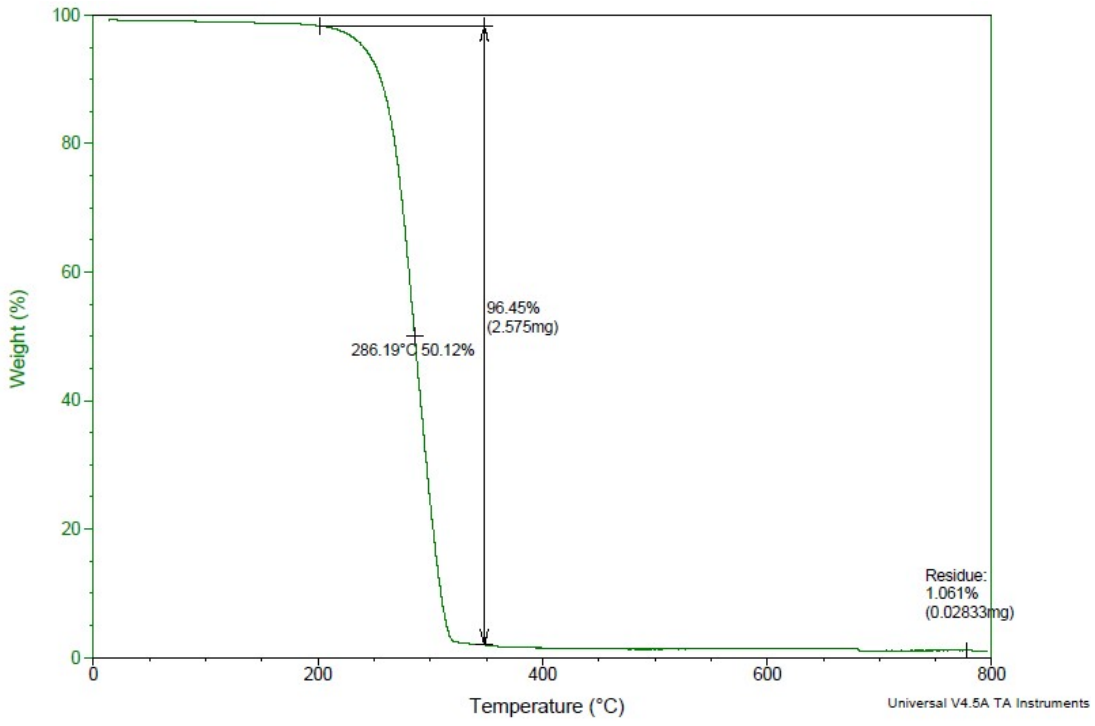

Figure S25. DSC thermogram for terpolymer **6** (Table S8, entry 6).